Radially Distorted Planar Motion Compatible Homographies

Marcus Valtonen Örnhag
Centre for Mathematical Sciences, Lund University, Lund, Sweden

Keywords: Planar Motion, Homography, Radial Distortion, Polynomial Solver, Trajectory Recovery, Visual Odometry.

Abstract: Fast and accurate homography estimation is essential to many computer vision applications, including scene degenerate cases and planarity detection. Such cases arise naturally in man-made environments, and failure to handle them will result in poor positioning estimates. Most modern day consumer cameras are affected by some level of radial distortion, which must be compensated for in order to get accurate estimates. This often demands calibration procedures, with specific scene requirements, and off-line processing. In this paper a novel polynomial solver for radially distorted planar motion compatible homographies is presented. The proposed algorithm is fast and numerically stable, and is proven on both synthetic and real data to work well inside a RANSAC loop.

1 INTRODUCTION

In many computer vision applications it is desired to find a homography between two images. Without imposing any prior knowledge of the model, or intrinsic parameters, a general homography can be estimated using a minimal of four point correspondences (Hartley and Zisserman, 2004). If any of the intrinsic parameters are known, or other model constraints are enforced, the number of needed point correspondences decrease, however, encoding these geometric properties may result in non-linear systems of polynomial equations. Solving such systems sufficiently fast, with an acceptable numerical precision, often involves methods from computational algebraic geometry (Cox et al., 2005).

Planar motion models are a well-studied field in computer vision. While several authors have considered restricted models, requiring various calibration procedures (Ortín and Montiel, 2001; Chen and Liu, 2006; Hajjdiab and Laganière, 2004), the general case, including the assumption of a constant—and unknown—overhead tilt, was introduced in (Liang and Pears, 2002). This model was also considered by (Wadenbäck and Heyden, 2013; Wadenbäck and Heyden, 2014; Zienkiewicz and Davison, 2015).

Many planar motion compatible navigation systems are based on estimating the homographies for consecutive views. Instead of eight degrees of freedom, as in the general case, planar motion compatible homographies only have five—two overhead tilt angles (assumed to be constant), one rotational angle, and two translational components. The standard procedure for estimating homographies is usually divided in extracting and matching keypoints, followed by estimating putative homographies in a robust framework. Typically, this is done using RANSAC in order to discard outliers introduced in the matching step. The probability of selecting a set of points containing only inliers depends on the amount of points selected, and therefore it is advantageous to make this choice minimal.

In this paper we consider the case of planar motion with a constant overhead tilt and unknown radial distortion. Such a setup is common for Visual Odometry (VO) in man-made environments, where the goal is to estimate the position of a vehicle, on which the camera is mounted. We propose a novel four point homography solver, which is suitable for real-time applications and numerically stable. The solver is compared to an existing solver and show an increase in performance on both synthetic and real data. Furthermore, we show how the solver can be incorporated in a VO pipeline for indoor navigation.

2 RELATED WORK

Consider a pair of point correspondences $\boldsymbol{x} \leftrightarrow \hat{\boldsymbol{x}}$, on a common scene plane, related by a homography $\boldsymbol{H}$. In homogeneous coordinates, let $\boldsymbol{x} = (x, y, w)^T$ and $\hat{\boldsymbol{x}} = (\hat{x}, \hat{y}, \hat{w})^T$, then $\lambda\hat{\boldsymbol{x}} = \boldsymbol{H}\boldsymbol{x}$, for some scalar λ. Left-

Örnhag, M.
Radially Distorted Planar Motion Compatible Homographies.
DOI: 10.5220/0008893802800288
In *Proceedings of the 9th International Conference on Pattern Recognition Applications and Methods (ICPRAM 2020)*, pages 280-288
ISBN: 978-989-758-397-1; ISSN: 2184-4313
Copyright © 2022 by SCITEPRESS – Science and Technology Publications, Lda. All rights reserved

multiplying this relation with the cross-product matrix $[\hat{\boldsymbol{x}}]_\times$ gives $[\hat{\boldsymbol{x}}]_\times \boldsymbol{H}\boldsymbol{x} = \boldsymbol{0}$, or, equivalently,

$$\begin{bmatrix} \boldsymbol{0} & -\hat{w}\boldsymbol{x}^T & \hat{y}\boldsymbol{x}^T \\ \hat{w}\boldsymbol{x}^T & \boldsymbol{0} & -\hat{x}\boldsymbol{x}^T \\ -\hat{y}\boldsymbol{x}^T & \hat{x}\boldsymbol{x}^T & \boldsymbol{0} \end{bmatrix} \begin{bmatrix} \boldsymbol{h}_1 \\ \boldsymbol{h}_2 \\ \boldsymbol{h}_3 \end{bmatrix} = \boldsymbol{0}, \qquad (1)$$

where $\boldsymbol{h}_k^T$ is the k:th row of the homography matrix $\boldsymbol{H}$. This formulation conveniently eliminates the scale parameter λ, while introducing two linearly independent equations, since the cross-product matrix is of rank 2. These are known as the *Direct Linear Transform* (DLT) equations. From this formulation, using four point correspondences, the minimal problem reduces to finding the one-dimensional null space of $\boldsymbol{H}$. If the homography is constrained further, as in the case of planar motion, this approach can still be used; however, the null space is no longer one-dimensional. The problem then translates into finding the corresponding null space basis coefficients. In (Wadenbäck et al., 2016) the authors showed that it was possible to construct a minimal solver for the general planar motion homography by using this approach, in which a polynomial system of 11 quartic equations in four variables are solved. Non-minimal relaxations of the same problem was studied in (Valtonen Örnhag, 2019), and tested in a VO framework for planar motion.

There are two common approaches for modeling radial distortion, the Brown–Conrady model (Brown, 1966), and the division model introduced in (Fitzgibbon, 2001). The latter has the benefit of being sufficiently good with fewer parameters than the former. We will exclusively use the division model with a single distortion parameter λ, in which the distorted (measured) image points are denoted $\boldsymbol{x}_i = \begin{bmatrix} x_i & y_i & 1 \end{bmatrix}^T$, and related to the undistorted image points $\boldsymbol{x}_i^u$, by the relation

$$\boldsymbol{x}_i^u = f(\boldsymbol{x}_i, \lambda) = \begin{bmatrix} x_i \\ y_i \\ 1 + \lambda(x_i^2 + y_i^2) \end{bmatrix}. \qquad (2)$$

where the distortion center is assumed to be at the center of the image, which is also the origin of our selected coordinate system. Since the distortion parameter only appears in the homogeneous coordinates, the DLT equations (1) still hold true, with the adjustment

$$[f(\hat{\boldsymbol{x}}_i, \lambda)]_\times \boldsymbol{H} f(\boldsymbol{x}_i, \lambda) = \boldsymbol{0}, \qquad (3)$$

for two point correspondences $\boldsymbol{x}_i \leftrightarrow \hat{\boldsymbol{x}}_i$. A minimal solver for the case of radially distorted homographies were presented in (Kukelova et al., 2015), in which the authors incorporated the radial distortion using the modified DLT equations (3). The same approach, but explicitly parameterizing the homography, have been used in (Pritts et al., 2018a), where the authors consider the case of conjugate translations. The case of jointly estimating lens distortion and affine rectification from coplanar features, was studied in (Pritts et al., 2018b). All the above methods reduce the problem to a polynomial system of equation for which the action matrix method is used (Cox et al., 2005). This typically involves finding a Gröbner basis, and extracting template coefficients in a finite field, which can be tedious manual work. Luckily, there are automatic solvers, such as the ones presented in (Kukelova et al., 2008a; Larsson and Åström, 2016; Larsson et al., 2017a; Larsson et al., 2017b; Larsson et al., 2018b), from which the above mentioned radially distorted homography solvers are derived.

An alternative to Gröbner basis methods is to view the problem as a Quadratic Eigenvalue Problem (QEP). This was done in (Fitzgibbon, 2001) and the same approach has been used by (Kukelova et al., 2008b; Kayumbi and Cavallaro, 2008).

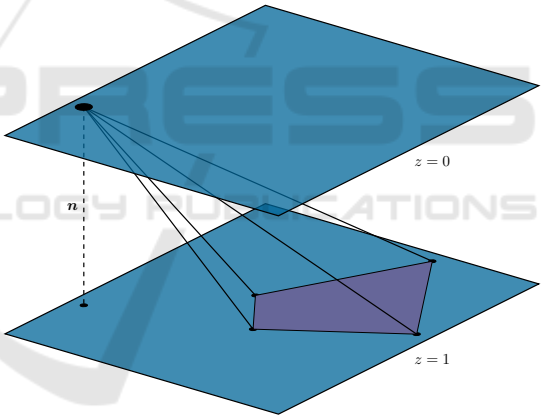

Figure 1: Illustration of the problem geometry. The ground plane is assumed to be positioned at $z = 1$, and the camera travels parallel in the plane $z = 0$. There are two unknown overhead tilt angles ψ (x-axis) and θi (y-axis), which are constant throughout the trajectory.

3 MODEL ASSUMPTIONS

We consider the original problem formulation in (Wadenbäck and Heyden, 2013), which assumes that a camera directed towards the floor is mounted on a vehicle. The scale of the global coordinate system is fixed by selecting the ground plane at $z = 1$, and the camera is assumed to travel parallel to the ground, in the plane $z = 0$, see Figure 1. Then, the camera matrices for two consecutive poses A and B, are given

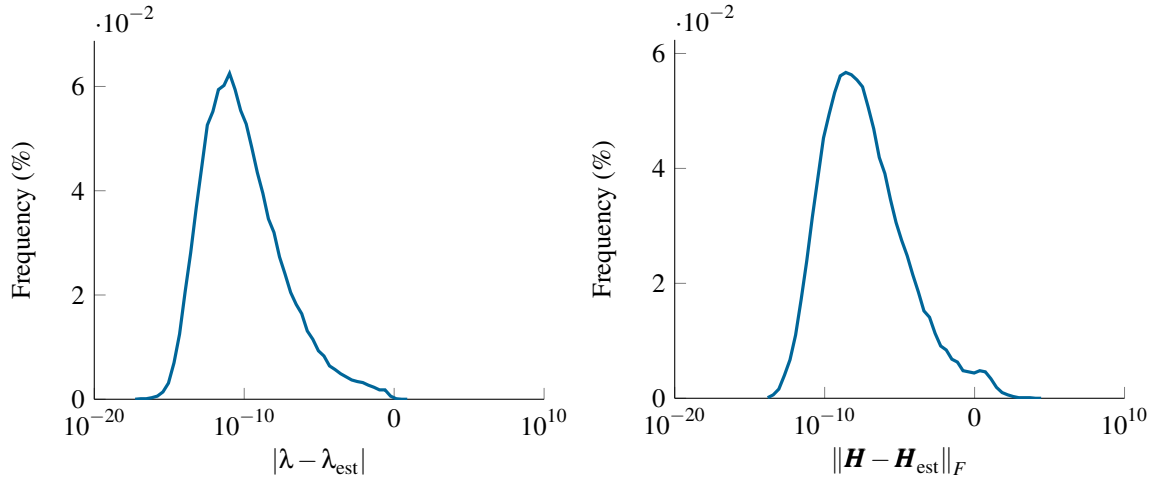

Figure 2: Error histogram the estimated distortion parameter λ (left) and the homography $\boldsymbol{H}$ for 100,000 random instances.

by

$$\begin{aligned} \boldsymbol{P}_A &= \boldsymbol{R}_{\psi\theta}[\boldsymbol{I} \mid \boldsymbol{0}], \\ \boldsymbol{P}_B &= \boldsymbol{R}_{\psi\theta}\boldsymbol{R}_{\phi}[\boldsymbol{I} \mid -\boldsymbol{t}], \end{aligned} \tag{4}$$

where $\boldsymbol{R}_{\psi\theta}$ is a rotation θ about the y-axis followed by a rotation of ψ about the x-axis. The vehicle may rotate about the z-axis by an angle ϕ, modeled by $\boldsymbol{R}_{\phi}$, and translate in the plane $z = 0$, thus leaving two translation components t_x and t_y. The corresponding homography is given by

$$\boldsymbol{H} = \lambda \boldsymbol{R}_{\psi\theta}\boldsymbol{R}_{\phi}\boldsymbol{T}_{\boldsymbol{t}}\boldsymbol{R}_{\psi\theta}^{T}, \tag{5}$$

where $\boldsymbol{T}_{\boldsymbol{t}} = \boldsymbol{I} - \boldsymbol{t}\boldsymbol{n}^T$ is a translation matrix, for the translation $\boldsymbol{t} = \begin{bmatrix} t_x & t_y & 0 \end{bmatrix}^T$, relative the plane normal $\boldsymbol{n} = \begin{bmatrix} 0 & 0 & 1 \end{bmatrix}^T$.

In (Wadenbäck et al., 2016) it was shown that a planar motion compatible homography $\boldsymbol{H}$ must fulfill 11 quartic constraints. Later, it was shown that by adding a sextic constraint, these conditions are both necessary and sufficient (Valtonen Örnhag, 2019).

4 NON-MINIMAL RELAXATION

Note that there are six degrees of freedom in the formulation—five in the planar motion compatible homography and one from the distortion parameter—hence using three points are required for the minimal configuration. This problem is surprisingly hard, and we have not found any tractable solution, which yields a solver sufficiently fast and stable for real-life scenarios. Instead, we propose a non-minimal relaxation, using four point correspondences. We argue that this compromise is acceptable, as the minimal case for a radially distorted general homography is 4.5 points (thus requiring 5 points in practice).

We draw inspiration from the approach in (Kukelova et al., 2015), however, we consider using only four point correspondences. By expanding the third row of (3), one obtains

$$\begin{aligned} (-\hat{y}_i h_{11} + \hat{x}_i h_{21})x_i + (-\hat{y}_i h_{12} + \hat{x}_i h_{22})y_i + \\ (-\hat{y}_i h_{13} + \hat{x}_i h_{23})w_i = 0, \end{aligned} \tag{6}$$

where $w_i = 1 + \lambda(x_i^2 + y_i^2)$ and $\hat{w}_i = 1 + \lambda(\hat{x}_i^2 + \hat{y}_i^2)$ are both functions of the radial distortion parameter λ. This is a homogeneous equation in eight monomials

$$\boldsymbol{v}_1 = \begin{bmatrix} h_{11} & h_{12} & h_{13} & h_{21} & h_{22} & h_{23} & \lambda h_{13} & \lambda h_{23} \end{bmatrix}^T. \tag{7}$$

With four point correspondences these can be stacked as

$$\boldsymbol{M}_1 \boldsymbol{v}_1 = \boldsymbol{0}, \tag{8}$$

where $\boldsymbol{M}_1$ is a 4×8 matrix, and $\boldsymbol{v}_1$ is defined as in (7). Hence, in general, the null space of $\boldsymbol{M}_1$ is four dimensional, and we may parameterize $\boldsymbol{v}_1$ as

$$\boldsymbol{v}_1 = \sum_{i=1}^{4} \gamma_i \boldsymbol{n}_i, \tag{9}$$

where γ_i are the new unknowns. To fix the scale we let $\gamma_4 = 1$. Since the elements of $\boldsymbol{v}_1$ are not independent, one needs to enforce two constraints, namely,

$$v_8 = \lambda v_6 \quad \text{and} \quad v_7 = \lambda v_3 \,. \tag{10}$$

Next, consider the second row of (3), which can be written

$$\boldsymbol{M}_2 \boldsymbol{v}_2 = \boldsymbol{0}, \tag{11}$$

where $\boldsymbol{M}_2 \in \mathbb{R}^{4\times 16}$, with the null space vector $\boldsymbol{v}_2$ consisting of 7 variables, and 16 monomials: h_{31}, h_{32}, h_{33}, λh_{33} and $\lambda^2\gamma_i$, $\lambda\gamma_i$, γ_i for $i = 1,2,3$ and λ^2, λ, 1. Since there are four equations with the same monomials we can eliminate the three first variables, h_{31}, h_{32}

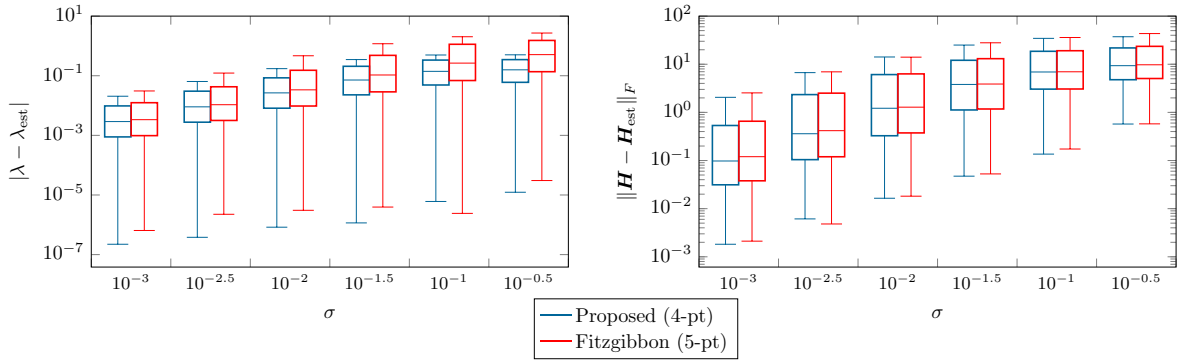

Figure 3: Distribution of estimation error in the distortion parameter λ, and the the homography $\boldsymbol{H}$ (measured in the Frobenius norm) for different noise levels σ. The proposed solver is compared to the five point solver (Fitzgibbon, 2001).

and h_{33}, using Gauss-Jordan elimination. Performing the elimination we obtain

$$\hat{\boldsymbol{M}}_2 = \begin{array}{c} \begin{array}{cccccccccccc} h_{31} & h_{32} & \lambda h_{33} & h_{33} & \lambda^2\gamma_1 & \lambda\gamma_i & \gamma_i & & \lambda^2 & \lambda & 1 \end{array} \\ \left[\begin{array}{cccccccccccc} 1 & & & & \bullet & \bullet & \bullet & \cdots & \bullet & \bullet & \bullet \\ & 1 & & & \bullet & \bullet & \bullet & \cdots & \bullet & \bullet & \bullet \\ & & 1 & & \bullet & \bullet & \bullet & \cdots & \bullet & \bullet & \bullet \\ & & & 1 & \bullet & \bullet & \bullet & \cdots & \bullet & \bullet & \bullet \end{array}\right] \end{array} \tag{12}$$

where we notice that the columns of the right 4×12 submatrix are not independent. In order to generate a correct solver, it is important to generate integer instances satisfying these dependencies.

From the eliminated system $\hat{\boldsymbol{M}}_2 \boldsymbol{v}_2 = \boldsymbol{0}$ we get the four equations.

$$\begin{aligned} h_{31} + f_1(\gamma_1,\gamma_2,\gamma_3,\lambda) &= 0, \\ h_{32} + f_2(\gamma_1,\gamma_2,\gamma_3,\lambda) &= 0, \\ \lambda h_{33} + f_3(\gamma_1,\gamma_2,\gamma_3,\lambda) &= 0, \\ h_{33} + f_4(\gamma_1,\gamma_2,\gamma_3,\lambda) &= 0, \end{aligned} \tag{13}$$

where $f_i(\gamma_1,\gamma_2,\gamma_3,\lambda)$ are polynomials in the variables γ_1, γ_2, γ_3, λ. Exploiting the relations between the last two equations of (13), an additional constraint is obtained

$$\lambda f_4(\gamma_1,\gamma_2,\gamma_3,\lambda) = f_3(\gamma_1,\gamma_2,\gamma_3,\lambda)\,. \tag{14}$$

The eliminated variables h_{31}, h_{32} and h_{33} are polynomials of degree three, thus making (14) of degree four. Together with (10) we have three equations in four unknowns. Since we are able to express all elements of the homography $\boldsymbol{H}$ as a function of four variables, we can enforce one of the 11 quartic constraints originally found in (Wadenbäck et al., 2016). Evaluating these constraints using $\boldsymbol{H}$ it turns out that ten of the constraints are of degree 12 and one of degree 10 due to cancellation of higher order terms. We choose the smallest one to build the polynomial solver.

Using the automatic generator (Larsson and Åström, 2016) we find that there are 18 solutions to the problem in general, and by sampling a basis based on the heuristic presented in (Larsson et al., 2018a) an elimination template of size 177×195 could be created.

5 EXPERIMENTS

5.1 Synthetic Data

The performance of the new polynomial solver is analyzed in terms of numerical stability and noise sensitivity. This is done by generating planar motion compatible homographies and distortion parameters. Scene points are generated and corresponding points are mapped using the previously generated homographies, followed by radially distorting the points using the division model.

The polynomial solver was generated according to Section 4 in C++, and the mean run-time is 0.73 ms (measured over 10,000 instances on a standard desktop computer).

5.1.1 Numerical Stability

We generate noise-free problem instances as described in the previous section, with physically reasonable parameters. As in (Kukelova et al., 2015) the distortion parameter λ was chosen in the interval $[-0.7, 0]$, which covers a wide range of distortions. The error histogram for 100,000 random instances are shown in Figure 2. The homographies were normalized such that $h_{33} = 1$. The majority of estimated distortion parameters λ are in the error range of 10^{-10} which is acceptable for most applications; however, there are still a significant parameter estimates of an error in the order of 10^{-2} or more, which is not negligible. This is likely to stem from

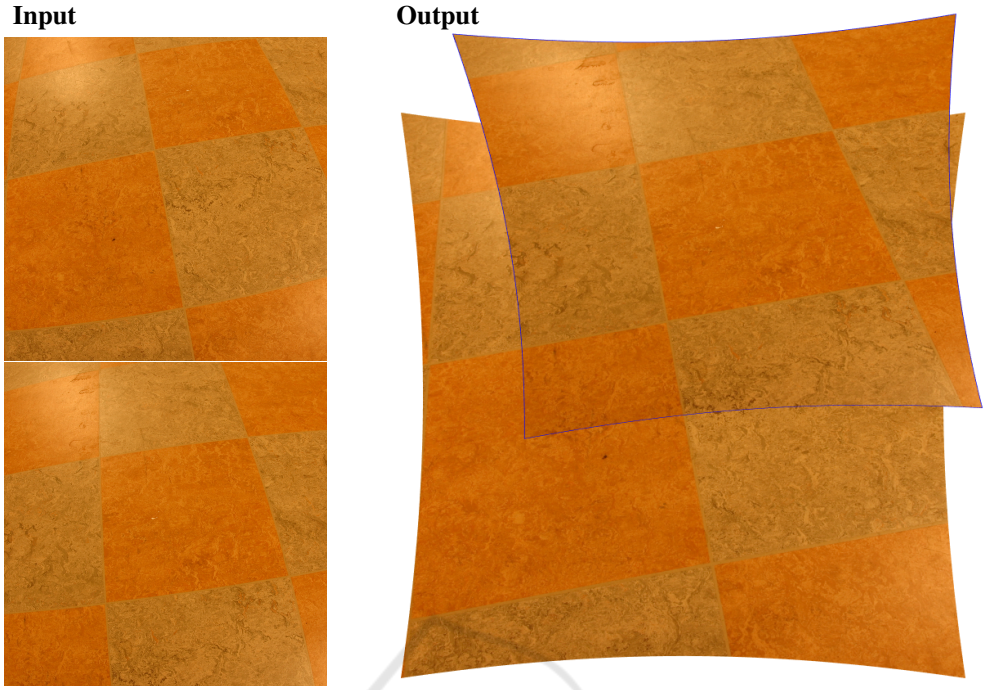

Figure 4: Two radially distorted images (left) and the rectified and stitched panorama. The distortion parameter and homography was obtained using the proposed solver in a RANSAC framework. Blue border added for visualization.

the ten degree polynomial, which increases the residual error notably. Nevertheless, we show that, carefully incorporated in a RANSAC framework, this is still a viable option to existing methods.

5.1.2 Noise Sensitivity

To analyze how well the solver copes with noise, the radially distorted image coordinates were corrupted by Gaussian noise with standard deviation σ, varying from mild to severe noise (in percent). The test was conducted 10,000 times per noise level, see Figure 3. As a comparison we use the five point method proposed in (Fitzgibbon, 2001). For all noise levels the mean error for the distortion parameter λ and the homography $\boldsymbol{H}$, obtained using the proposed solver, are lower compared to the five point method.

5.2 Real Images

5.2.1 Image Stitching

Stitching of images is a classic problem in computer vision. In this section, we show that the proposed method yields a visually acceptable output from real data.

The images were taken using a digital camera with a fish-eye lens mounted on a tripod, see Figure 5. The overhead tilt was kept fixed and the entire tripod moved along the floor, thus creating a planar motion compatible homography between the images.

Figure 5: Setup used in the panorama stitching experiment.

We use a standard approach for estimating the homography. First we detect and extract SURF keypoints, followed by matching them using the nearest neighbor algorithm. Outliers are removed in a RANSAC framework. No non-linear refinement of the obtained homography was performed. The final

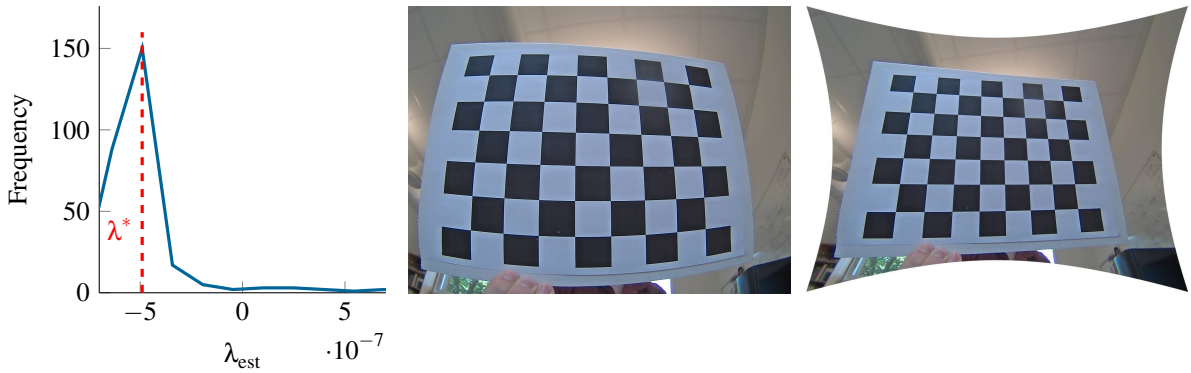

Figure 6: (Left) Histogram of estimated distortion parameters for the proposed method evaluating during the *parallel parking* sequence. The selected parameter λ^* is marked with a dashed line. (Middle) Undistorted image of a calibration chart, not part of the sequence. (Right) Rectified image using the estimated parameter λ^*.

panorama can be seen in Figure 4. Note that the lines appear straight in the final output, indicating that the radial distortion parameter has been correctly estimated. In Figure 7 we compare the number of inliers vs. number of RANSAC iterations for the same image pair, using the proposed method and the five point solver in (Fitzgibbon, 2001). In the experiment we mean-value the number of inliers over 500 problem instances, and the proposed method consistently has a higher number of inliers.

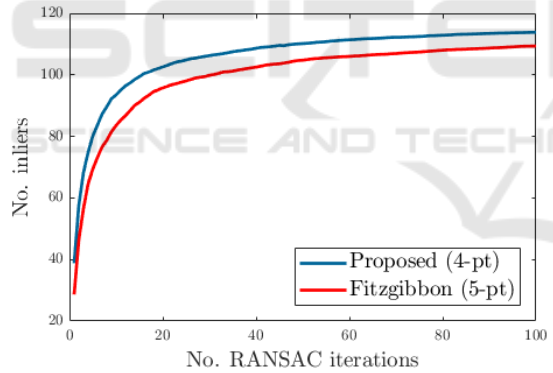

Figure 7: Number of inliers vs. number of RANSAC iterations for the images in Figure 4. The data has been mean-valued over 500 test instances.

5.2.2 Application to Visual Odometry

In this final section we show that the proposed solver can be incorporated in a VO pipeline to achieve better performance to the compared method. The classic pipeline consists of constructing an initial solution for the camera poses, intrinsic parameters and scene points, and then refine these using Bundle Adjustment (BA). In general, if a better initial solution can be obtained, fewer iterations of BA are needed for the same performance. As the latter step often amounts in a large optimization step, it is certainly advantageous to decrease the number of necessary iterations.

In this experiment we use the data from the mobile robot experiment in (Wadenbäck et al., 2017). The robot is equipped with omnidirectional wheels (Fraunhofer IPA rob@work) and has a camera (with visible radial distortion) mounted downwards, such that the floor is predominantly in the field of view. Reference images of a calibration pattern (checkerboard) are taken as a sanity check of the estimated distortion parameter. Furthermore, a reference system with an absolute accuracy of 100 μm is set up to track the platform, from which the ground truth data is obtained.

The robot is programmed with three sequences, described below:

Line. Forward motion in a straight line with a constant orientation (320 images),

Turn. Forward motion while rotating, resulting in a slight turn (344 images),

Parallel Parking. Forward motion followed by a sharp turn, while keeping constant rotation (325 images).

As in the stitching experiment in the previous section we compare the proposed method to the one in (Fitzgibbon, 2001). For each pair of consecutive images a homography and a radial distortion parameter are estimated using both methods. Then the method in (Wadenbäck and Heyden, 2014) is used to recover the full set of motion parameters. From these the trajectory of the robot is extracted and compared to the ground truth, see Figure 8. Both methods perform well, with a slight preference for the proposed method. This result is consistent with the findings in (Valtonen Örnhag, 2019); namely, that pre-optimization on an early stage in the VO pipeline, does not lead to a significant performance boost. This is, in large, due to the constraint that the constant overhead tilt throughout the entire trajectory cannot be enforced on a single homography alone, but rather

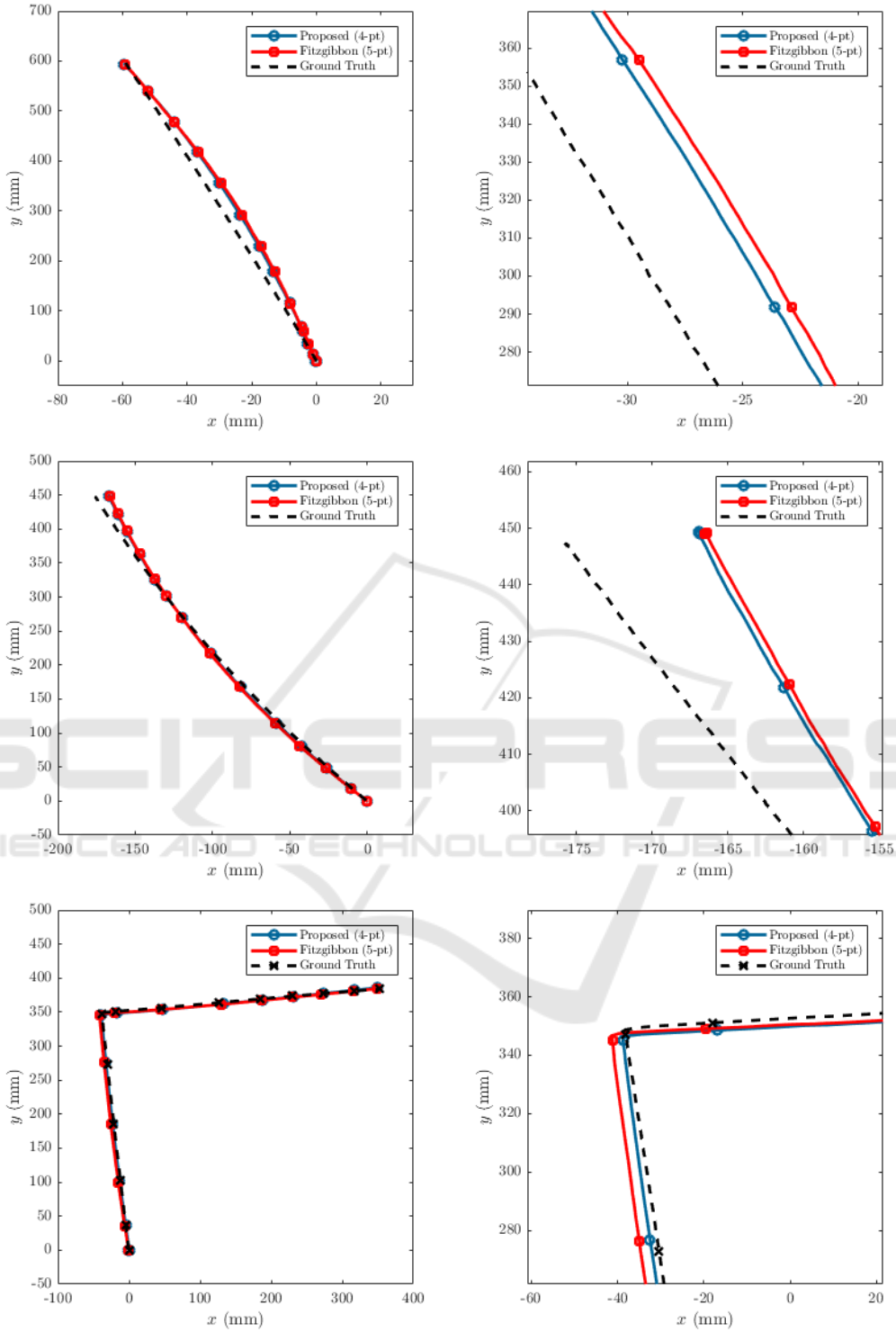

Figure 8: Estimated trajectories for *line*, *turn* and *parallel parking* of the VO experiment in Section 5.2.2. Images to the left show the entire trajectory, and the ones to the right are zoomed in on a region of interest.

requires a sequence of homographies. Nevertheless, there is still the same performance gain in terms of the number of RANSAC iterations needed to acquire a given inlier ratio, as was demonstrated in Section 5.2.1.

The presented experiment does not enforce the

same radial distortion parameter throughout the trajectory of the robot, as it estimates a new parameter along with each homography. In order to enforce the same radial distortion compensation, we may use histogram voting of the estimated distortion parameters. In Figure 6 we have done so for the estimated parameters acquired during the *parallel parking* test sequence. The most likely parameter λ^* is then used to rectify a previously unseen image of the calibration scene. While the rectified image is not perfect, it may serve as a good initial solution for further non-linear refinement.

6 CONCLUSIONS

One cannot ignore radial distortion when estimating trajectories in a Visual Odometry framework. In this paper we have considered radially distorted homographies compatible with the general planar motion model. We have proposed a novel algorithm for estimating the homographies and showed on both real and synthetic data that it increases the performance compared to a general homography estimation method with radial distortion. Furthermore, we show, by incorporating the proposed algorithm in a VO pipeline, that it yields satisfactory results in terms of estimating the radial distortion parameter.

ACKNOWLEDGMENTS

The author gratefully acknowledges Mårten Wadenbäck and Martin Karlsson for providing the data for the planar motion compatible sequences, and Magnus Oskarsson for fruitful discussions regarding the basis selection heuristic which made the proposed solver faster. This work has been funded by the Swedish Research Council through grant no. 2015-05639 'Visual SLAM based on Planar Homographies'.

REFERENCES

Brown, D. C. (1966). Decentering distortion of lenses. *Photogrammetric Engineering*, 32:444–462.

Chen, T. and Liu, Y.-H. (2006). A robust approach for structure from planar motion by stereo image sequences. *Machine Vision and Applications (MVA)*, 17(3):197–209.

Cox, D. A., Little, J., and O'Shea, D. (2005). *Using Algebraic Geometry*. Graduate Texts in Mathematics. Springer New York.

Fitzgibbon, A. W. (2001). Simultaneous linear estimation of multiple view geometry and lens distortion. In *Conference on Computer Vision and Pattern Recognition (CVPR)*.

Hajjdiab, H. and Laganière, R. (2004). Vision-based multi-robot simultaneous localization and mapping. In *Canadian Conference on Computer and Robot Vision (CRV)*, pages 155–162, London, ON, Canada.

Hartley, R. I. and Zisserman, A. (2004). *Multiple View Geometry in Computer Vision*. Cambridge University Press, Cambridge, England, UK, second edition.

Kayumbi, G. and Cavallaro, A. (2008). Multiview trajectory mapping using homography with lens distortion correction. *EURASIP Journal on Image and Video Processing*, page 145715.

Kukelova, Z., Bujnak, M., and Pajdla, T. (2008a). Automatic generator of minimal problem solvers. *European Conference on Computer Vision (ECCV)*, pages 302–315.

Kukelova, Z., Bujnak, M., and Pajdla, T. (2008b). Polynomial eigenvalue solutions to the 5-pt and 6-pt relative pose problems. In *British Machine Vision Conference (BMVC)*.

Kukelova, Z., Heller, J., Bujnak, M., and Pajdla, T. (2015). Radial distortion homography. In *Conference on Computer Vision and Pattern Recognition (CVPR)*, pages 639–647.

Larsson, V. and Åström, K. (2016). Uncovering symmetries in polynomial systems. *European Conference on Computer Vision (ECCV)*, pages 252–267.

Larsson, V., Åström, K., and Oskarsson, M. (2017a). Efficient solvers for minimal problems by syzygy-based reduction. *Computer Vision and Pattern Recognition (CVPR)*, pages 2383–2392.

Larsson, V., Åström, K., and Oskarsson, M. (2017b). Polynomial solvers for saturated ideals. *International Conference on Computer Vision (ICCV)*, pages 2307–2316.

Larsson, V., Kukelova, Z., and Zheng, Y. (2018a). Camera pose estimation with unknown principal point. *Computer Vision and Pattern Recognition (CVPR)*, pages 2984–2992.

Larsson, V., Oskarsson, M., Åström, K., Wallis, A., Kukelova, Z., and Pajdla, T. (2018b). Beyond gröbner bases: Basis selection for minimal solvers. *Computer Vision and Pattern Recognition (CVPR)*, pages 3945–3954.

Liang, B. and Pears, N. (2002). Visual navigation using planar homographies. In *International Conference on Robotics and Automation (ICRA)*, pages 205–210, Washington, DC, USA.

Ortín, D. and Montiel, J. M. M. (2001). Indoor robot motion based on monocular images. *Robotica*, 19(3):331–342.

Pritts, J., Kukelova, Z., Larsson, V., and Chum, O. (2018a). Radially-distorted conjugate translations. In *Conference on Computer Vision and Pattern Recognition (CVPR)*.

Pritts, J., Kukelova, Z., Larsson, V., and Chum, O. (2018b).

Rectification from radially-distorted scales. In *Asian Conference of Computer Vision (ACCV)*, pages 36–52.

Valtonen Örnhag, M. (2019). Fast non-minimal solvers for planar motion compatible homographies. In *International Conference on Pattern Recognition Applications and Methods (ICPRAM)*, pages 40–51, Prague, Czech Republic.

Wadenbäck, M. and Heyden, A. (2013). Planar motion and hand-eye calibration using inter-image homographies from a planar scene. *International Conference on Computer Vision Theory and Applications (VISAPP)*, pages 164–168.

Wadenbäck, M. and Heyden, A. (2014). Ego-motion recovery and robust tilt estimation for planar motion using several homographies. *International Conference on Computer Vision Theory and Applications (VISAPP)*, pages 635–639.

Wadenbäck, M., Karlsson, M., Heyden, A., Robertsson, A., and Johansson, R. (2017). Visual odometry from two point correspondences and initial automatic tilt calibration. In *International Joint Conference on Computer Vision, Imaging and Computer Graphics Theory and Applications (VISIGRAPP 2017)*, pages 340–346.

Wadenbäck, M., Åström, K., and Heyden, A. (2016). Recovering planar motion from homographies obtained using a 2.5-point solver for a polynomial system. *International Conference on Image Processing (ICIP)*, pages 2966–2970.

Zienkiewicz, J. and Davison, A. J. (2015). Extrinsics autocalibration for dense planar visual odometry. *Journal of Field Robotics (JFR)*, 32(5):803–825.

SCITEPRESS
SCIENCE AND TECHNOLOGY PUBLICATIONS